

Preparation and investigation of the structural and optical characteristics of manganese- doped cadmium oxide films

A. A. Mohammed* M. A. Ahmed, S. M. Jassim
The general for Education in Diyala, Diyala, Iraq

In this paper, undoped and Mn-doped CdO thin films deposited on the glass substrates by the chemical spray pyrolysis method (CSP) technique. The prepared thin films characterized by XRD, AFM, FESEM and UV visible. The results of the X-ray diffraction patterns revealed that the prepared films have a polycrystalline structure and a cubic structure. The crystallite size (D) value for all prepared films was calculated using Scherrer's method, Williamson-Hall method and size strain plot (SSP) method, from the results, it was observed that, the crystallite size decreases with increase in doping ratio of Manganese. The optical properties show that with an increase in Mn concentration, the CdO films' transparency and the energy gap of the films increases. The Hall effect measurement revealed that all prepared films have negative type (n-type) charge carriers, the value of the doping ratio rises, the Hall coefficient decreases.

(Received January 21, 2023; Accepted April 24, 2023)

Keywords: CdO, Chemical spray pyrolysis, Thin films, Structural properties, Hall effect

1. Introduction

Cadmium oxide is known as an inorganic compound. The element cadmium can be obtained (industrially) from the intense heating of pure cadmium in the air and to a certain temperature (below its melting point). And ammonia salts, while it has no solubility in water or bases [1]. Cadmium oxide has two forms (structural formulas) in nature: crystalline and random, and its crystalline structure is characterized as brown or red, while its random structural form is colorless [2]. Its crystal structure is described as having a face-centered cubic (Fcc), crystal structure similar to that of sodium chloride (NaCl) [3], This means that a single ordinary unit cell of a crystal of the compound contains four lattice points, each of the lattice points is accompanied by a base consisting of two ions, one of which is the positive cadmium ion (Cd^{+2}) and the other is the negative oxygen ion (O^{-2}) [4]. Thus, one normal unit cell includes two positive Cd ions and four negative O ions [4]. Four molecules of cadmium oxide, the positive cadmium ions occupy the eight heads of the cubic cell and the centers of its six faces, while the negative oxygen ions occupy the center and the middles of its 12 sides [5]. CdO is a part of the periodic table's (II - VI) group, and it has an energy gap of (2.16–2.6 eV) at room temperature (300 K) [5,6]. Several studies have been conducted on the preparation of undoped and doped cadmium oxide. N. MANJULA et al. [2] studied the effect of Mn-doped CdO thin films, the results showed that, Mn doping concentration reduces film crystallite size from 34.63 nm to 17.68 nm and optical band gap. S. Dugan et al. [7] prepared undoped and Mn doped CdO using sol-gel method and deposited on Si substrate, the optical properties showed that bandgap energies between 2.41 eV and 1.70 eV. K.Kasiraja et al. [8] prepared undoped and Mn doped CdO using spray pyrolysis method, the optical properties showed that, the bandgap values drop with doping concentration (2.51, 2.47, and 2.21 eV) and increase with higher concentrations (2.37 eV). P.Sakthivel et al. [9] prepared CdO thin films using radio frequency magnetron sputtered, the AFM pictures of the CdO thin films demonstrated that the roughness of the films increased with the deposition time, and the FESEM analysis revealed that the film deposited for 30 min was very uniform nanopyramidal structures. I. M. Mohammed et al. [10] prepared CdO thin films with different Mn-doping using spray pyrolysis method, the optical properties showed that, the depending on the Mn content, the bandgap ranges from 2.60 eV to 2.50 eV. The aim of this work is synthesize $\text{Cd}_{1-x}\text{Mn}_x\text{O}$ thin films at $x = (0, 3, 5, 7 \text{ and } 9 \%)$, and study

*Corresponding author: aalmudaris8@gmail.com
<https://doi.org/10.15251/DJNB.2023.182.613>

the effect of Mn-doped on some of the structural, optical and electrical properties of CdO thin films.

2. Experimental details

Chemical spray pyrolysis method is utilized to synthesize $\text{Cd}_{1-x}\text{Mn}_x\text{O}$ films at $x = (0, 3, 5, 7 \text{ and } 9 \%)$ using materials: Cadmium nitrate $[\text{Cd}(\text{NO}_3)_2 \cdot 4\text{H}_2\text{O}]$, molecular weight (308.47 g/Mol) and density (8.15g/cm, in addition, at a concentration of 0.1M in the (100 ml), it is a solid substance (powder) that dissolves quickly in water and is white in color. Manganese acetate was used with the chemical formula $[\text{Mn}(\text{CH}_3\text{COO})_2 \cdot 4\text{H}_2\text{O}]$, its molecular weight (g/mol) 173.027 and its density (1.74 g/cm³). It is a powder in light pink color. As a solution of aqueous manganese acetate with a molar concentration of (0.1M) was prepared by dissolving (0.271.73) of it in (100ml) of distilled water prepared for this purpose, where the required weight was obtained using the mathematical relationship (3-1) using a scale with sensitivity (10^{-4}g) mix the solution well using a magnetic stirrer for 60 min to ensure complete dissolution and homogeneity of the solution.

3. Results and discussions

3.1. Structural analysis (xrd)

The structural characterization of undoped CdO and Mn-doped CdO films were carried out using x-ray diffraction technique. The spray pyrolysis process was used to deposit undoped and Mn-doped CdO films, as shown in Fig.1. All of the patterns were found to have diffraction peaks about ($2\theta = 33.77^\circ, 38.22^\circ, 55.26^\circ, 65.86^\circ$ and 69.46°) referred to (111), (200), (220), (311) and (222) favorite planes respectively [11]. The ICDD card number agrees with the outcome (005-0640). The strongest peak is at (111) plane ($2 = 33.77^\circ$). Increased Mn dopant intensified the (111) plane. Well-crystalline films have strong and crisp diffraction peaks. The diffraction peaks of the produced samples matched those of the cubic crystalline structure, indicating that the samples are polycrystalline. The absence of Mn-related impurity phase diffraction peaks in the XRD spectra shows Mn doping does not modify the crystal structure and Mn incorporation into CdO via replacement for Cd [12]. XRD spectra of Mn-doped CdO films indicate a minor change in peak location toward lower angles due to Mn^{2+} substitution in the host lattice [13]. Table 1 shows Scherrer's relation results for all produced films' crystallite size (D) [14].

$$D = \left(\frac{k\lambda}{\beta \cos\theta} \right) \quad (1)$$

where D is the crystallite size, K is a constant (equal to 0.94), λ is the wavelength of the x-ray radiation, β is the full width at half maximum and θ is the angle of diffraction. From the results, it was observed that with an increase in Mn concentration, the crystallite size value decreases. The films have crystallite sizes on the order of a nanometer. The Mn-doped CdO films' status as nanomaterials is thus confirmed. The crystallite size and micro strains of the prepared films were also calculated using the Williamson-Hall method according below equation [15]:

$$\beta_{(hkl)} \cos\theta = \left(\frac{k\lambda}{D} \right) + 4S \sin\theta \quad (2)$$

where, $\beta_{(hkl)}$ is full width of half maximum, k is constant, D is the size of the crystallite, λ is the wavelength, θ is the Bragg's angle, and S is the microstrain. Strain and crystallite size may be determined from the slope and y-intercept of the fitted line, respectively, as illustrated in Fig. 2, if $\beta_{(hkl)} \cos\theta$ is plotted with respect to $4 \sin\theta$, with the use of a small amount of strain, it is discovered that the diffracting domains are isotropic. The size-strain plot (SSP) procedure, which is used in the isotropic line extension example, can provide a superior evaluation. The benefit is that high-angle reflection data is given less weight [16]. The connection between strain, expanding peak, and crystallite size [17].

$$(d \beta \cos \theta)^2 = \left(\frac{\kappa}{D}\right)^2 d^2 \beta \cos \theta + \left(\frac{\epsilon}{2}\right)^2 \quad (3)$$

where κ is the form factor, which in spherical geometry is equal to 3/4. Fig. 3 illustrates how to create the line equation Eq. (6) as $(d \beta \cos \theta)^2$ against $(d^2 \beta \cos \theta)$. As demonstrated in Fig. 3, the slope of the line may be used to compute the crystallite size (D). Table 1 contains the results. It was noted that the values of the crystallite size for the CdO thin films (doped and un-doped) in these findings qualitatively concur with the results of the crystallite size obtained using the Williamson-Hall technique, as given in Table 1. There were no discernible differences in the XRD patterns of any of the produced films. The variable displacements of the atoms from their reference lattice location during sample development are what cause the micro strain in the samples [11]. All synthetic films had positive micro strain values, which suggests that lattice dispersion has taken place [18].

Table 1. Data for the X-ray diffraction of the thin films of CdO with and without Mn doping.

Thin films	2 θ (deg.)	FWHM (deg.)	plane (hkl)	D (nm) (Scherrer method)	D (nm) (W-H method)	D (nm) (SSP method)	Micro Strain (10^{-4})
Undoped-CdO	33.77	0.71000	111	50.09	54.16	40.68	1.077
CdO: Mn (3%)	32.97	0.16780	111	49.4	61.9	42.48	3.036
CdO: Mn (5%)	33.01	0.17810	111	46.5	57.29	40.73	1.85
CdO: Mn (7%)	33.03	0.16480	111	45.08	68.64	38.13	3.8
CdO: Mn (9%)	33.066	0.18390	111	40.92	70.38	31.23	4.27

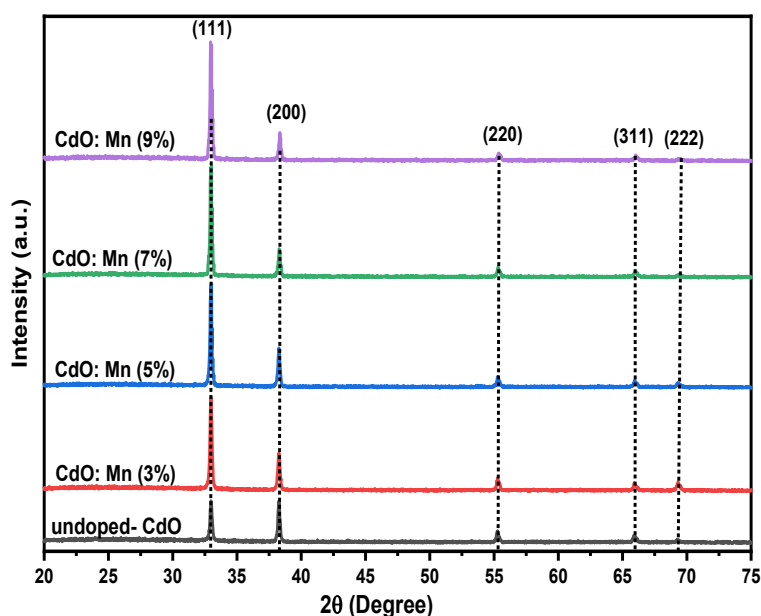


Fig. 1. Undoped and Mn-doped CdO thin films' XRD patterns.

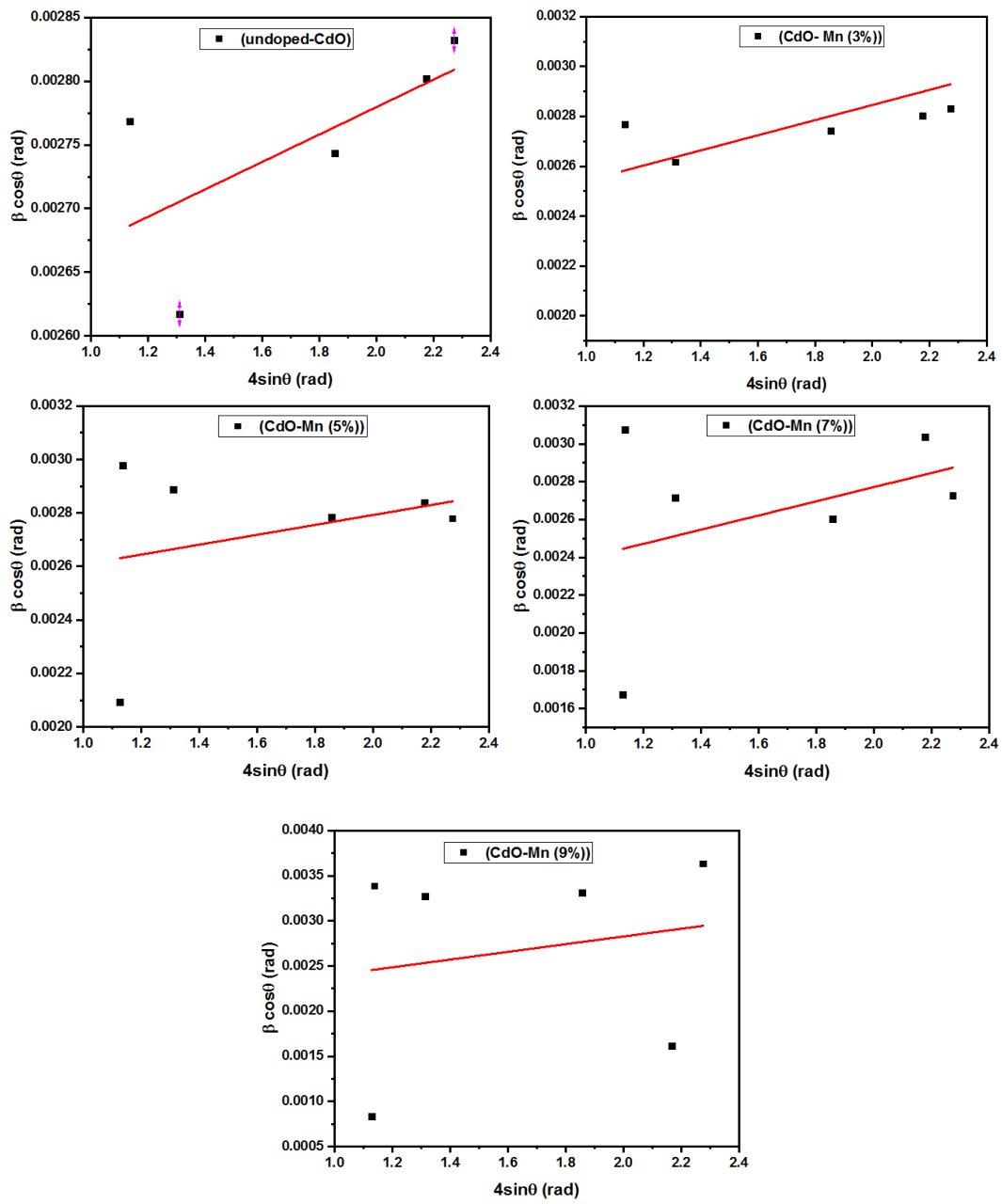


Fig. 2. *W-H* study of Mn-doped and undoped CdO films.

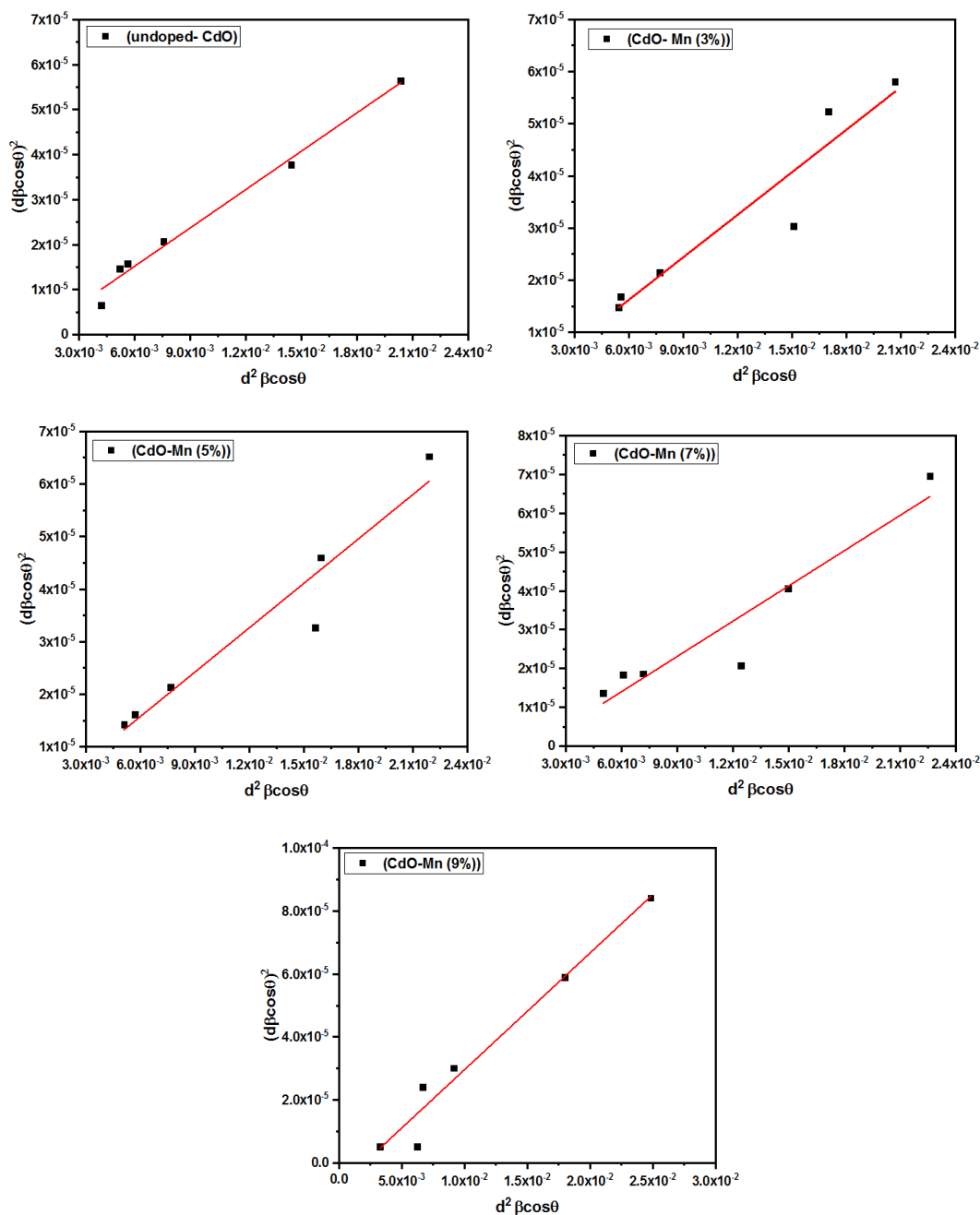


Fig. 3. The SSP analysis of undoped and Mn-doped CdO films.

3.2. Optical properties

The transmittance spectra of the Mn-doped and undoped CdO films, which were recorded in the (200-1000 nm) wavelength range, are shown in Figure 4. The transparency ranges from 30 to 98 percent in the visible range, as shown in Fig. 4. The Mn-dopant improves the transparency of the CdO films in the visible range, and this change in transparency denotes a regular shift in dopant. Because it is generally known that variations in transmittance rely on the film's material properties, this shift in transparency is connected to those materials' structural aspects [19]. After Mn doping, it was observed that the transmittance greatly increased as a result of a minor shift in the absorption edge (blue shift) [20]. This suggests that the optical band gap of the CdO films is increased by the Mn dopant. The equation [21, 22] is used with Tauc's model to calculate the optical band gap of all produced films:

$$\alpha h\nu = R (h\nu - E_g)^m \quad (4)$$

where R is a constant that is independent of photon energy and has four numerical values (1/2 for allowed direct, 2 for allowed indirect, 3 for forbidden direct, and 3/2 for forbidden indirect optical transitions), h is the photon energy, E_g is the optical band gap, and α is the absorption coefficient [23]. In Fig. 5, the Tauc's plot of CdO thin films made with various Mn-doping concentrations is displayed. The produced films' E_g values (undoped and Mn-doped) are listed in Table 2. Table 2 shows that as the Mn dopant concentration rises, the films' E_g values do as well.. The Cd^{2+} ions in the CdO lattice may have been successfully replaced with Mn^{2+} ions, increasing the band gap. An increase in carrier concentration and mobility is what is responsible for the blue shift (Burstein-Moss effect) [24] of the doped CdO absorption edge.

Table 2. Energy band gap of the undoped and Mn-doped CdO films as a function of Mn concentration.

Samples	E_g (eV)
Undoped-CdO	2.26
CdO: Mn (3%)	2.47
CdO: Mn (5%)	2.60
CdO: Mn (7%)	2.71
CdO: Mn (9%)	2.84

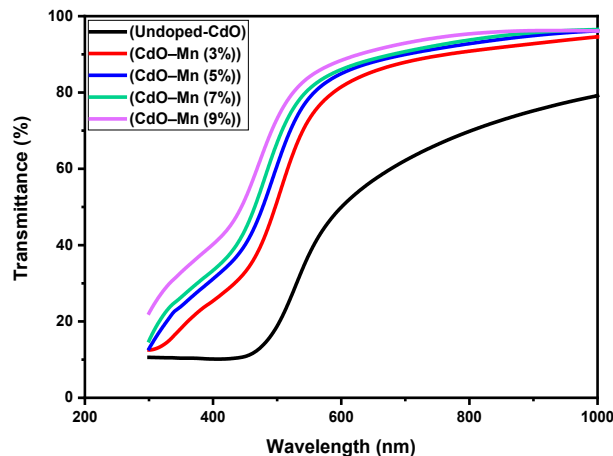


Fig. 4. Transmittance spectra of undoped and Mn-doped CdO films.

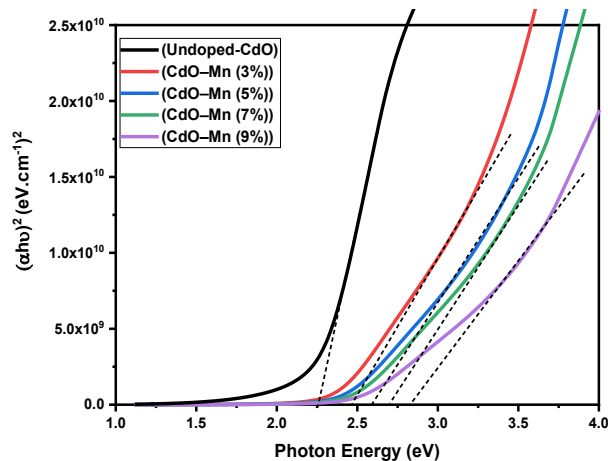
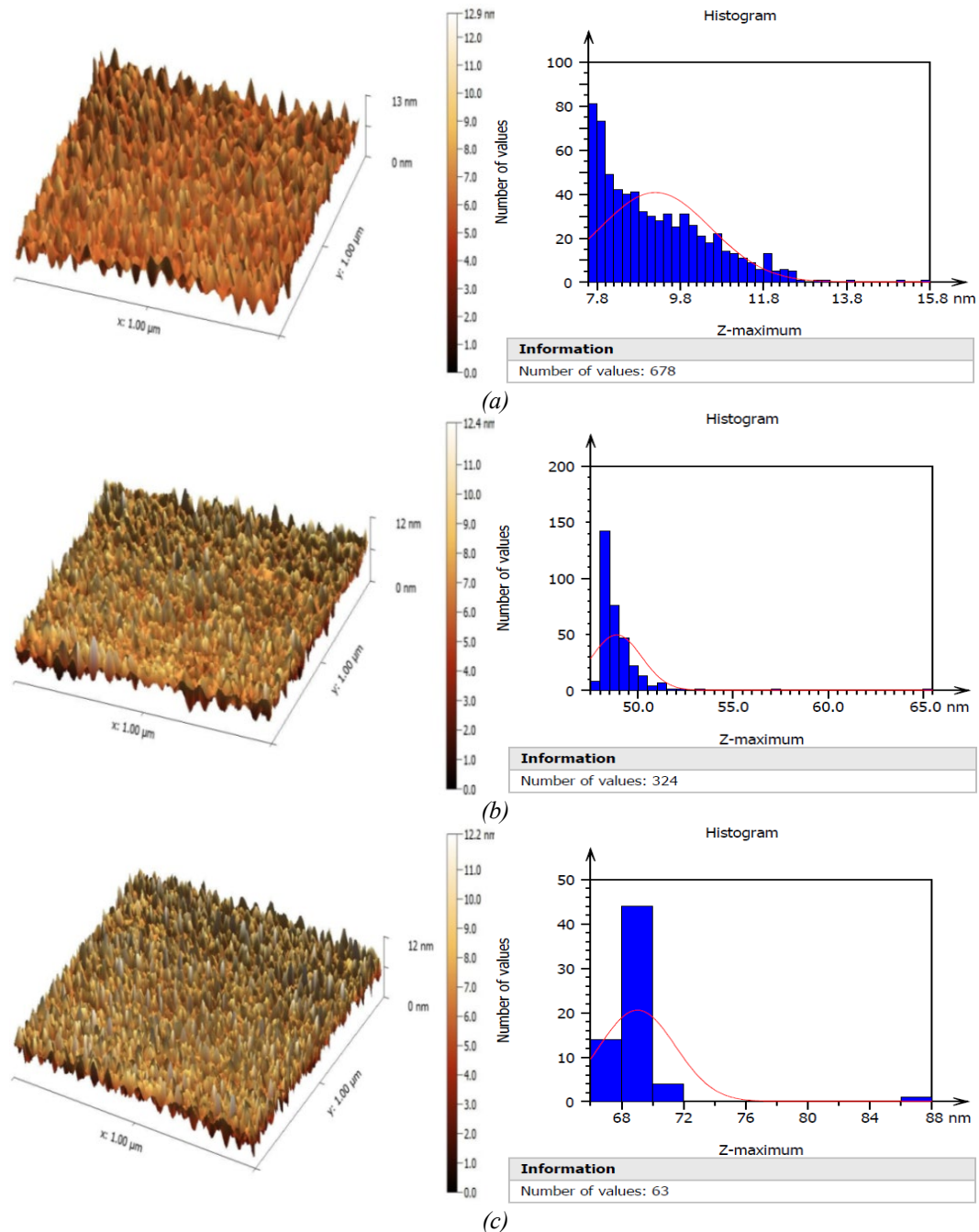


Fig. 5. Tauc's plot of undoped and Mn-doped CdO films.

3.3. Analysis of AFM

Figure 6 (a and b) and (c, d, e and f) respectively show the (AFM) surface 3D images of the (MnO, CdO pure) and doped by (3 thin film deposited on a glass substrate at various substrate temperatures). When the Mn concentration is increased from 3% to 9%, the distribution of grains is uniform on the substrate surface. Because of the increased radical mobility on the sample surface, an improvement in surface roughness was observed [10]. Surface roughness values also rise in tandem with an increase in mean square root, as shown in table 3.



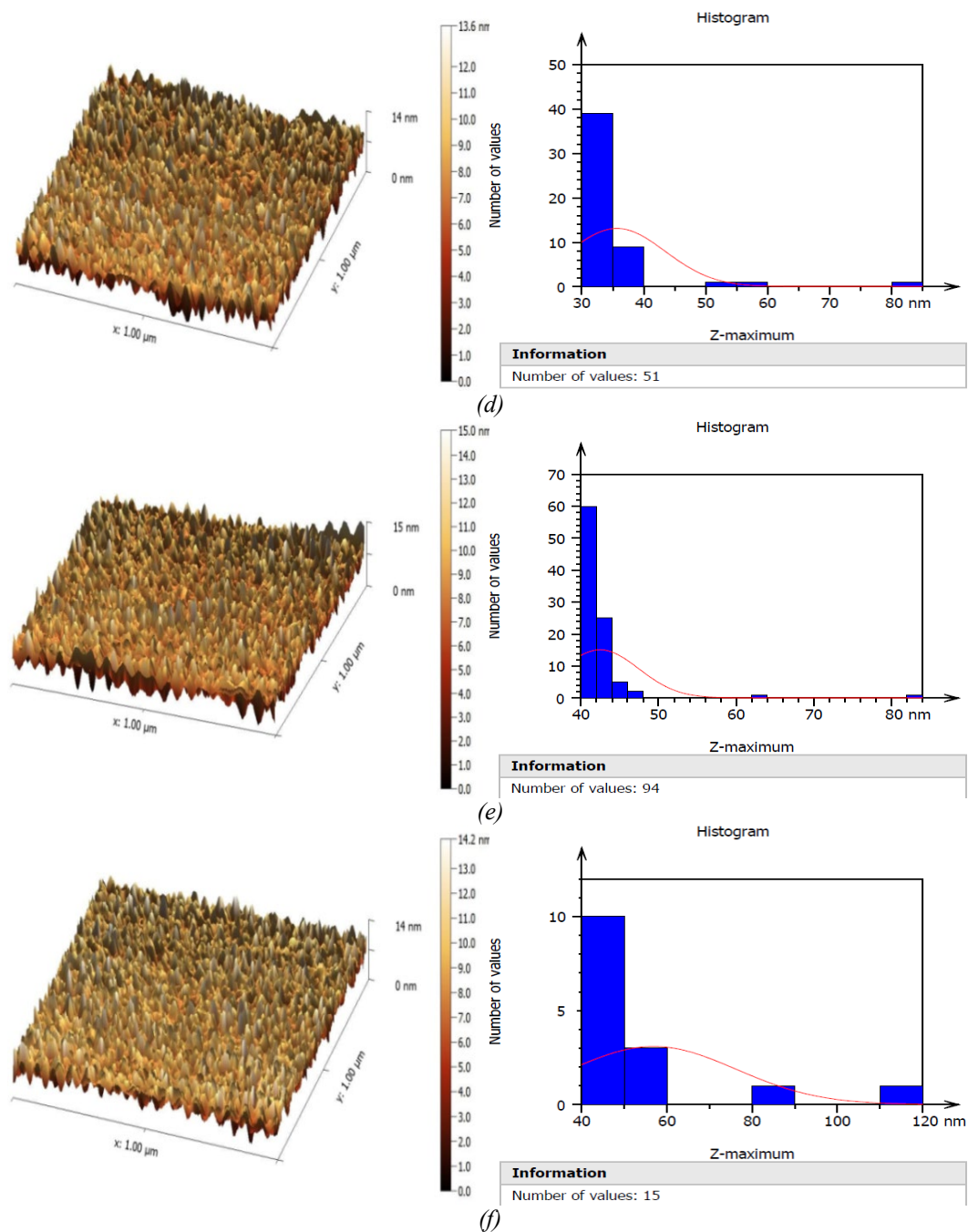


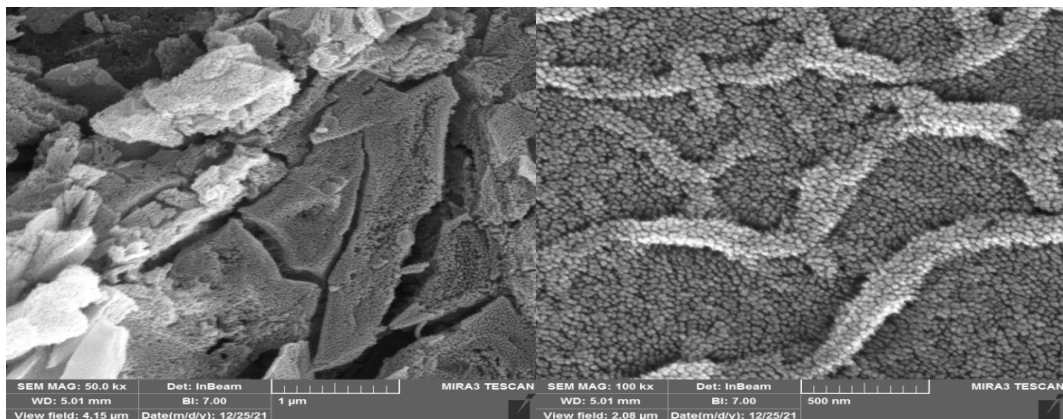
Fig. 6. AFM images of a) MnO, b) undoped CdO and (c,d, e and f) Mn-doped CdO thin films.

Table 3. Surface roughness, mean roughness square, and particle size.

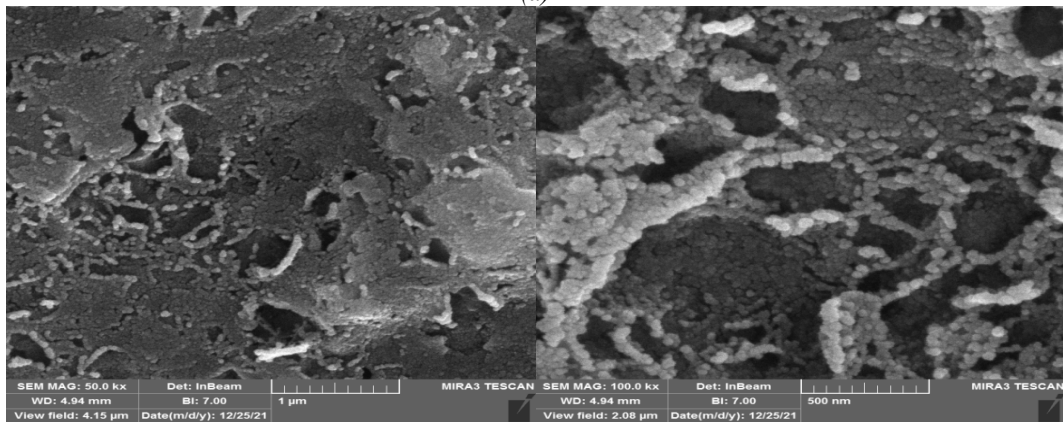
Sample	Grain size (nm)	Surface roughness (nm)	RMS (nm)
CdO pure	9.201	1.793	1.889
MnO pure	48.87	6.026	7.682
CdO:Mn _{0.03}	69.03	7.721	14.63
CdO:Mn _{0.05}	35.67	9.738	17.90
CdO:Mn _{0.07}	42.46	9.147	15.12
CdO:Mn _{0.09}	56.83	14.00	29.15

3.4. Analysis of FESEM

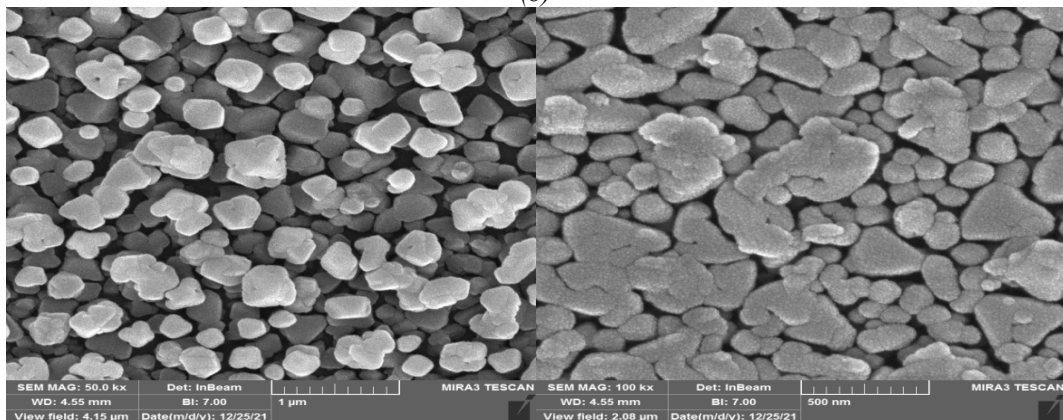
The surface morphology of the CdO: Mn thin films prepared by spray pyrolysis methods were investigated at different molar ratios (3%, 5%, 7%, and 9%) of Mn. Fig.7 a represents images of a film of (MnO) where we notice that the surface is homogeneous and with a uniform distribution of particles on the base with some voids on the surface and nanoparticles have spherical shapes and different sizes, while Fig.7 b It represents a film (CdO) where the surface appears irregular with few gaps and the nanoparticles have spherical shapes and different sizes, and there is some agglomeration. Fig.7 (c, d, and e) illustrates images of Mn-doped CdO films, it was noted that the surface in general is irregular and consists of stereotypes with different surfaces and topped with small semi-spherical grains, and this is evidence of the effect of the grafting material. While, Fig.7 f shows the image of the membrane with (CdO: 9%Mn) doped ratio, which has a uniform and needle-shaped surface.



(a)



(b)



(c)

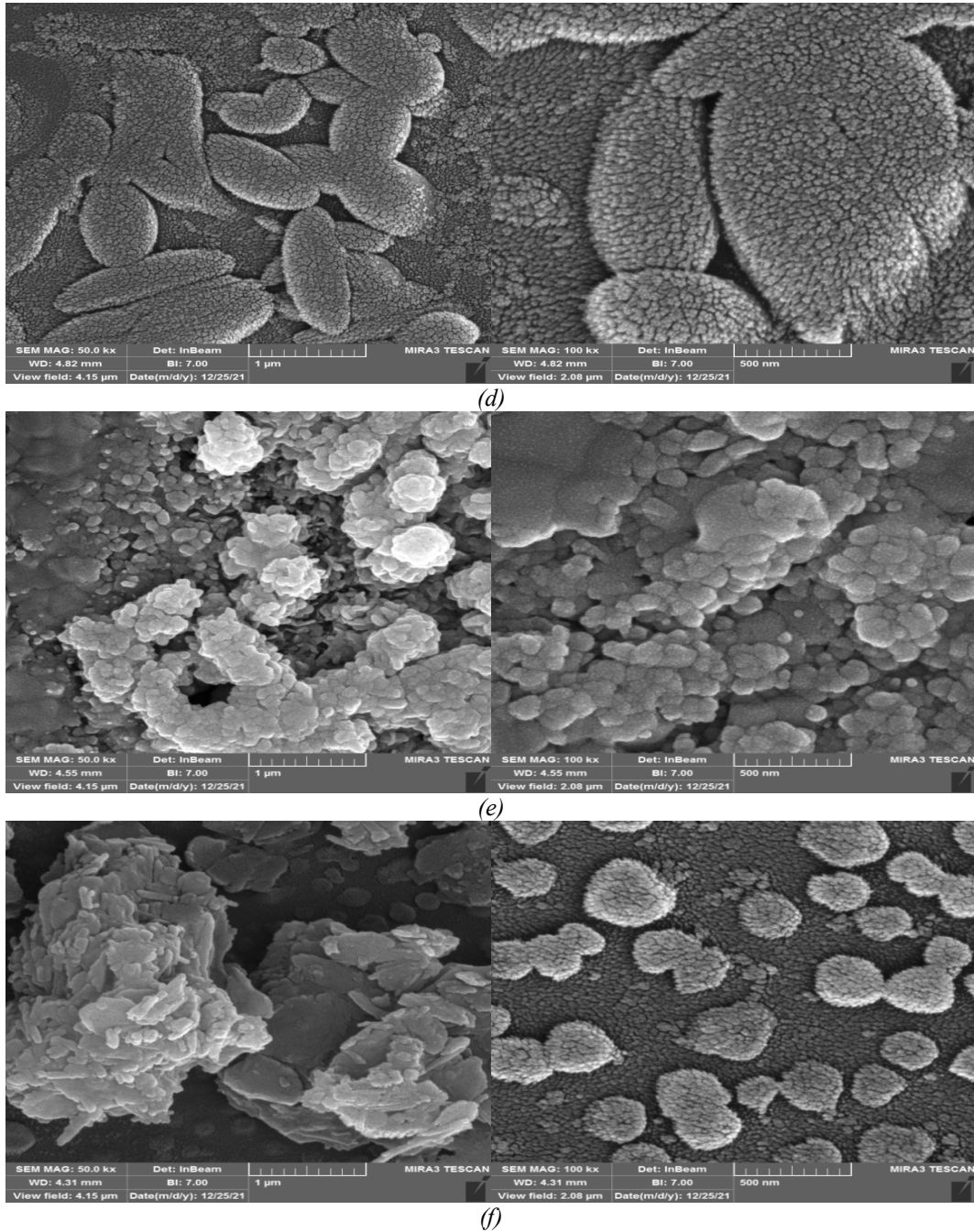


Fig. 7. FESEM images of a) MnO, b) undoped CdO and (c,d, e and f) Mn-doped CdO thin films.

3.5. Hall Effect measurement

The Hall effect measurement was carried out at room temperature and by the effect of a uniform magnetic field of intensity (0.55T) of undoped CdO and Mn-doped CdO thin films, with doping percentages (3, 5, 7 and 9 %) as clear values of Hall coefficient (R_H), the concentration of the majority charge carriers (n), the values of each of the mobility (μ_H) and electrical conductivity (σ) as shown in Table 4. From the negative sign associated with the value of the Hall coefficient, it is clear that the type of charge carriers is of the negative type (n-type) for all prepared films, as the quality of the charge carriers was not affected by vaccination [4]. The table 4 shows that the value of the Hall coefficient decreases with the increase of doping, as there was an increase in the electron concentration values (n) as shown in fig.8, which was accompanied by a decrease in mobility (μ_H) with an increase in the rates of inoculation with manganese when the temperature

was constant, as shown in fig.9 and Table 4. These results confirm that increasing the inoculation percentage caused an increase in donor levels, which in turn resulted in an increase in the concentration of (Mn) atoms and leads to its entry as compensatory atoms to the oxygen spaces as well, and the formation of bonds with cadmium, which causes a decrease in the oxygen spaces and thus causes a decrease in the electrical conductivity [25]. While the decrease in mobility can be explained by the increase in doping has led to a decrease in the average free path time (τ), which in turn results in a slight decrease in the value of mobility compared to the clear increase in the concentration of electrons, which is responsible for the increase in conductivity at constant temperature [26, 27]. These results indicate the possibility of using these films with negative Hall coefficient in solar cell applications, gas sensors and other application.

Table 4. Results of the Hall effect experiment of undoped and Mn-doped CdO thin films.

Samples	R_H (cm^3/C)	$n \times 10^{20}$ (cm^{-3})	μ_H ($\text{cm}^2/\text{V.S}$)	ρ ($\Omega.\text{cm}$)	σ ($\Omega.\text{cm}$) ⁻¹
Undoped-CdO	-6.22	1.522	6.88	0.71659	0.9131833
CdO: Mn (3%)	-5.62	1.733	6.74	0.833828	1.199288
CdO:Mn (5%)	-5.47	2.521	5.898	0.927433	1.078245
CdO: Mn (7%)	-4.348	2.426	3.811	1.140908	0.876495
CdO: Mn (9%)	-4.775	2.805	2.235	2.136465	0.468063

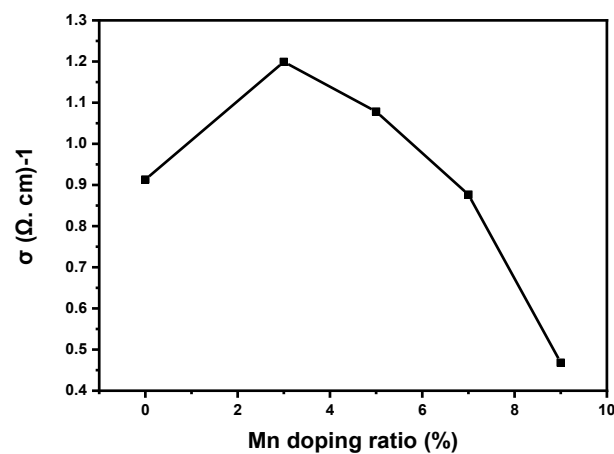


Fig. 8. Variation of Hall conductivity of undoped and Mn-doped CdO thin films.

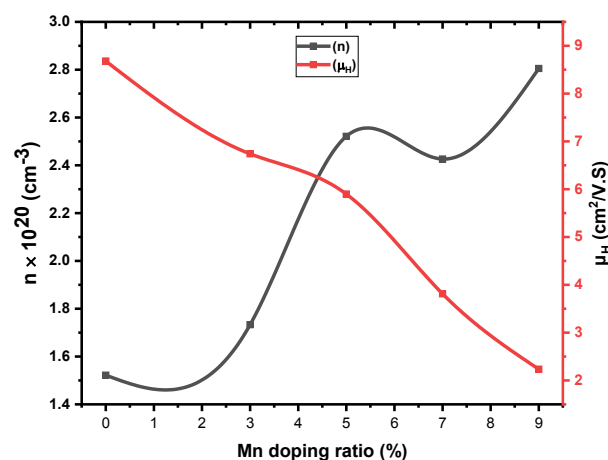


Fig. 9. Variation of the concentration and Hall mobility of the charge carriers of Mn-doped CdO thin films.

4. Conclusions

Undoped and Mn-doped CdO thin films prepared by the chemical spray pyrolysis method (CSP) technique at $x = 0, 0.03, 0.05, 0.07$ and 0.09% . XRD patterns showed that the thin films have a polycrystalline and a cubic structure and the crystallite size decreases with increase in Mn doping. The optical properties show that the transparency and energy gap of the CdO films increases with an increase in Mn doping. The Hall effect measurement showed that the type of charge carriers is of the negative type (n-type) for all prepared films, the value of the Hall coefficient decreases with the increase of doping.

References

- [1] R. K. Gupta, K. Ghosh, R. Patel, P. K. Kahol, *Physica E: Low-dimensional Systems and Nanostructures* 44(1), 163(2011); <https://doi.org/10.1016/j.physe.2011.08.009>
- [2] Manjula, N., Pugalenth, M., Nagarethinam, V. S., Usharani, K., & Balu, A. R., *Mater. Sci. Poland*, 33(4), 774 (2015); <https://doi.org/10.1515/msp-2015-0115>
- [3] Gürbüz, E., Aydın, R., & Şahin, B., *Journal of Materials Science: Materials in Electronics*, 29(3), 1823 (2018); <https://doi.org/10.1007/s10854-017-8091-z>
- [4] Bian, Y., Bian, Z. Y., Zhang, J. X., Ding, A. Z., Liu, S. L., & Wang, H., *Applied Surface Science*, 329, 269 (2015); <https://doi.org/10.1016/j.apsusc.2014.12.090>
- [5] Smart, L. E., & Moore, E. A. (2012). *Solid state chemistry: an introduction*. CRC press.
- [6] Azeroual, H., Bantignies, J. L., Alvarez, L., Maurin, D., Granier, D., Haines, J., Hermet, P., *Journal of Materials Chemistry C*, 10(25), 9499 (2022); <https://doi.org/10.1039/D2TC00769J>
- [7] Dugan, S., Koç, M. M., Coşkun, B., *Journal of Molecular Structure*, (1202), 127 (2020); <https://doi.org/10.1016/j.molstruc.2019.127235>
- [8] Kasirajan, K., Anasthasiya, A. N. A., Aldossary, O. M., Ubaidullah, M., Karunakaran, M., *Structural, Sensors and Actuators A: Physical*, 319(4) 125(2021); <https://doi.org/10.1016/j.sna.2020.112531>
- [9] Sakthivel, P., Murugan, R., Asaithambi, S., Karuppaiah, M., Rajendran, S., Ravi, G., *Journal of Physics and Chemistry of Solids*, 126, 1(2019); <https://doi.org/10.1016/j.jpics.2018.10.031>
- [10] Mohammed, I. M., Abood, Z. M., & Chaid, S. S., *J. for Engineering and Science*, 3, 70 (2020).
- [11] Alahmed, Z. A., Albrithen, H. A., Al-Ghamdi, A. A., Yakuphanoglu, F., *Optik*, 126(5) 575(2015); <https://doi.org/10.1016/j.ijleo.2015.01.005>
- [12] M. Xin, L. Z. Hu, D. Liu, and N. Yu, *Superlattices and Microstructures*, 74, 234 (2014); <https://doi.org/10.1016/j.spmi.2014.06.009>
- [13] Z. B. Bahsi, and A. Y. Oral, *Optical Materials*, 29(6), 672 (2007); <https://doi.org/10.1016/j.optmat.2005.11.016>
- [14] A. K. Ali, N. A. Bakr, Sh. M. Jassim, *J. Photon. Mater. Tech.* 2, 20 (2016).
- [15] A. A. Mohammed, Z. T. Khodair, and A. A. Khadom, *Chemical Data Collections*, 29, 100531, (2020); <https://doi.org/10.1016/j.cdc.2020.100531>
- [16] N. M. Khatir, Z. A. Malek, A. K. Zak, A. Akbari, F. Sabbagh, *Journal of Sol-Gel Science and Technology*, 78 (1), 98 (2016).
- [17] A. K. Zak, W. A. Majid, M. E. Abrishami, and R. Yousefi, *Solid State Sciences*, 13(1), 251(2011); <https://doi.org/10.1016/j.solidstatesciences.2010.11.024>
- [18] Z. T. Khodair, Anees A. Khadom, Hassan A. Jasim, *Journal of Materials Research and Technology*, 8(1), 424 (2019); <https://doi.org/10.1016/j.jmrt.2018.03.003>
- [19] N. Mahdi, and N. Bakr, *East European Journal of Physics*, 3, 84 (2022); <https://doi.org/10.26565/2312-4334-2022-3-11>
- [20] M. Anitha, N. Anitha, K. Saravanakumar, I. Kulandaisamy, L. Amalraj, *Applied Physics A*, 124 (8), 1 (2018); <https://doi.org/10.1007/s00339-018-1993-7>

- [21] Sh. Jassim, N. Bakr, F. Mustafa, J. Mater. Sci. Mater. Elect. 31, 16199 (2020);
<https://doi.org/10.1007/s10854-020-04084-1>
- [22] Z. T. Khodair, N. A. Bakr, A. M. Hassan, A. A. Kamil, Journal of Ovonic Research, 15(6), 377- (2019).
- [23] Sh. M. Jassim, Journal of Electronic Materials, 51(6), 2828 (2022);
<https://doi.org/10.1007/s11664-022-09562-2>
- [24] A. K. Sharma, S. S. Potdar, K. S. Pakhare, U. M. Patil, V. S. Patil, M. C. Naik, Journal of Materials Science: Materials in Electronics, 31(23), 20932 (2020);
<https://doi.org/10.1007/s10854-020-04607-w>
- [25] K. Usharan and A. R Balu, Acta Metall. Sinica, 28(1), 64(2015);
<https://doi.org/10.1007/s40195-014-0168-6>
- [26] E. Makori, I. Amatalo, P. Karimi, W. Njoroge, Int. J. Optoelectron. Eng., 4, (1), 11(2014).
- [27] Kasirajan, K., Anasthasiya, A. N. A., Aldossary, O. M., Ubaidullah, M., Karunakaran, M., Sensors and Actuators A: Physical, 319, 125(2021);
<https://doi.org/10.1016/j.sna.2020.112531>